

# Comparison of Potential Flow and Viscous Fluid Models in Gap Resonance

Lin LU<sup>1</sup>, Liang CHENG<sup>2</sup>, Bin TENG<sup>3</sup>, Liang SUN<sup>4</sup>

<sup>1</sup> Center for Deepwater Engineering, Dalian University of Technology, China. [LuLin@dlut.edu.cn](mailto:LuLin@dlut.edu.cn)

<sup>2</sup> School of Civil and Resource Engineering, The University of Western Australia, Australia

<sup>3</sup> State Key Laboratory of Coastal and Offshore Engineering, Dalian University of Technology, China

<sup>4</sup> Centre for Offshore Research and Engineering, National University of Singapore, Singapore

## Abstract

This work presents numerical simulation results of wave motion in narrow gaps subjected to incident water waves using both potential theory flow model and viscous fluid model, including single narrow gap separated by twin bodies and double narrow gaps between three identical bodies. The numerical results of variation of wave height in the narrow gaps with incident wave frequencies are compared with available experimental data. The numerical results and comparisons indicated that both potential flow model and viscous fluid model are able to predict the resonant frequency. However, it was found that potential flow model significantly over-predict the wave height in narrow gaps at frequencies near the resonant frequency. It was revealed that the viscous effect/or energy dissipation plays an important role in limiting the wave height in narrow gaps at resonance. The mechanism of fluid forces on structures is also investigated based on the numerical simulations using the viscous fluid model.

## Key words

Fluid Resonance, Narrow Gap, Potential Flow Model, Viscous Fluid Model, Boundary Element Method, Finite Element Method

## Introduction

Multiple floating structures arranged side by side with small separations are commonly used in oil and gas offloading facilities, such as a LNG tank berthing adjacent to a FPSO or wharf. The characteristic dimensions of the gaps between the neighboring structures are usually very small compared with that of the individual structure. When the multi-floating structures with narrow gaps are subject to water waves the phenomena of fluid resonance may take place, which can lead to very large amplitudes of wave oscillations in the narrow gaps and increase of wave forces on the structures at resonance frequencies. The onset condition of fluid resonance, the resonant wave height in narrow gaps and the magnitude of wave forces on structures are of engineering significance. Therefore, many efforts have been made with emphasis on these aspects, such as the laboratory tests, theoretical analysis and numerical investigations. The numerical models developed so far are mainly based on the potential flow theory (Miao et al., 2001, Li et al. 2005, Zhu et al., 2008). It is speculated that pure potential flow models may over-predict the wave amplitudes in the narrow gaps since the fluid viscosity and energy dissipations can not be taken into

account by potential flow models. Alternatively, some attempts of introducing artificial damping to overcome this difficulty of potential flow models (Chen et al., 2005, Pauw et al. 2007). This method works well in limiting the amplitude of water oscillations in the narrow gap. However the specification of damping coefficients for real applications remains a challenge for those models. The main purpose of this work is to model the fluid resonance in narrow gaps within the frame of viscous fluid theory such that the crucial energy dissipation involving the fluid resonance can be investigated.

## Numerical models

The viscous numerical model is composed of a three-step finite element solver for Navier-stokes equations, an internal wave maker for wave generation, a CLEAR Volume of Fluid (CLEAR-VOF) technique for free surface capture and a spongy layer for reducing reflected waves.

Flow of incompressible viscous Newtonian fluids is governed by the continuity equation and Navier-Stokes equations,

$$\frac{\partial u_i}{\partial x_i} = \begin{cases} q(\mathbf{x}, t) & \mathbf{x} \in \Omega_s \\ 0 & \mathbf{x} \notin \Omega_s \end{cases} \quad (1)$$

$$\frac{\partial u_i}{\partial t} + u_j \frac{\partial u_i}{\partial x_j} = -\frac{1}{\rho} \frac{\partial p}{\partial x_i} + \nu \frac{\partial}{\partial x_j} \left( \frac{\partial u_i}{\partial x_j} \right) + f_i + \frac{\nu}{3} \frac{\partial q}{\partial x_i} \quad (2)$$

where,  $u_i$  and  $f_i$  are the velocity and body forces components in the  $i$  direction and  $p$ ,  $\rho$  and  $\nu$  denote the pressure, fluid density and kinematic viscosity, respectively. In Eq. (1), a source term  $q(\mathbf{x}, t)$  is activated in the source region  $\Omega_s$  to generate desirable waves by means of internal wave maker. The governing equations are solved by an upwind finite element method. Details of numerical discretization and validations can be found in Lu et al. (2008) and Lu et al. (2009). Free surface oscillations induced by resonance in narrow gaps are captured by the CLEAR-VOF method, which is inherently consistent with the finite element method and irregular mesh partition. An artificial spongy layer is employed to reduce the reflected waves by means of incorporating a vertical resistance in the body force term.

The potential theory model is based on assumptions that the fluid flow is incompressible, inviscid and irrotational. The governing equation for incompressible, inviscid and irrotational flow is described by Laplace Equation of the velocity potential  $\Phi(x, y, t)$  as,

$$\Delta \Phi = 0 \quad (3)$$

Equation (3) is solved with appropriate boundary conditions using the boundary element method. Details

of the model can be found in Sun et al. (2008). In the present study, only the first order results are concerned.

## Numerical results

The viscous numerical wave flume was applied first to investigate the fluid resonance in a narrow gap between twin bodies. The numerical results on the variation of wave heights in the narrow gap with incident wave frequencies are then compared with available experimental data. According to the laboratory tests of Saitoh et al. (2006), two identical boxes with breadth  $B=50$  cm are fixed in a wave flume with water depth  $h=50$  cm. The incident wave heights range from 2.3 cm to 2.5 cm in the experiments, while a uniform incident wave height  $H_0=2.4$  cm is adopted in the numerical investigations. Two cases with different draft  $D$  and gap width  $B_g$  are considered here. They are  $D=25.2$  cm with  $B_g=5$  cm and  $D=15.3$  cm with  $B_g=7$  cm, respectively. The computational domain is divided into nearly 200,000 un-uniform rectangular meshes. A sketch definition of the numerical set-up is shown in Fig. 1.

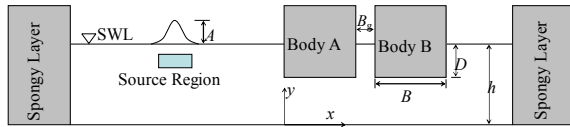


Fig. 1 Sketch definition of the viscous numerical wave flume

Fig. 2 shows a typical example of the time-series of wave oscillations in the narrow gap at three wave lengths  $L=2.0$  m, 1.7 m and 1.5 m for the case of  $D=25.2$  cm and  $B_g=5$  cm.

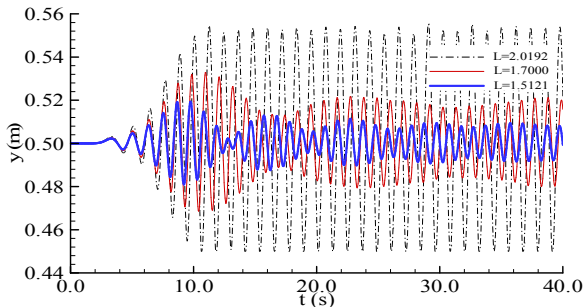
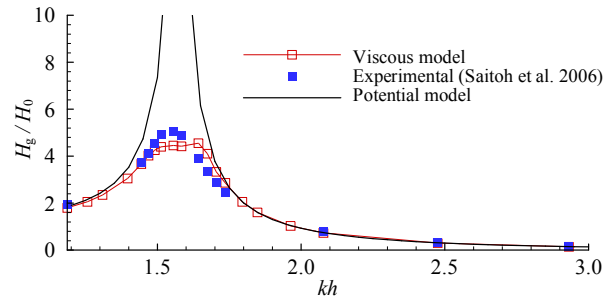


Fig. 2 Evolution of free surface in the narrow gap with different incident wave conditions

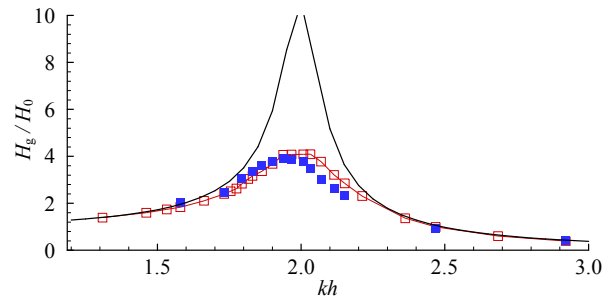
It was found that regular wave motions are established rather quickly for incident waves of wave length  $L=2.02$ , while free surface elevations in the narrow gap for incident waves of  $L=1.70$  m and 1.51 m appear to be of typical beating characteristics with different oscillation frequencies and amplitudes. The large amplitude oscillations in the narrow gap for incident waves of wave length  $L=2.02$  were clearly due to the flow resonance because the incident wave frequency is very close to the natural frequency of the system ( $kh=1.56$ ). The beating phenomena observed for incident waves of  $L=1.70$  m and 1.51 m are caused by the superposition of oscillations of different frequencies. One of the two dominant frequencies involved is the incident wave frequency and the other is the natural frequency of fluid-structure system. It is quite obvious

that no resonance took place under these two incident wave frequencies. This is the reason why wave amplitudes in the narrow gap under these two incident wave frequencies are much smaller than that with  $L=2.02$  m.

The variations of averaging wave height  $H_g/H_0$  in the narrow gap with respect to the wave number  $kh$  are plotted in Fig. 3 (a) and (b) for the two cases of  $D=25.2$  cm with  $B_g=5$  cm and  $D=15.3$  cm with  $B_g=7$  cm, respectively. For the purpose of comparison, the experimental data of Saitoh et al. (2006) and the potential flow solutions are also included in these figures. It can be seen from Fig. 3 (a) that the viscous numerical results of amplitude of free surface oscillation in the narrow gap agrees well with the experimental data. Fig. 3 (a) shows that the resonant frequency predicted by viscous model,  $kh=1.556$ , is almost identical to that obtained in laboratory tests. While the maximum wave height from the viscous wave flume is  $H_g/H_0=4.46$ , which is slightly smaller than that observed in experiments. In contrast, the numerical results of resonant wave height from the potential flow model are much higher than the experimental data. The good performance of viscous flow numerical model is demonstrated again in Fig. 3 (b), where the different draft and gap width are considered. The comparisons of numerical results of viscous and potential flow models with experimental data show that the viscous flow model works very well and is able to produce accurate predictions for not only the resonant frequency but also the wave heights in the narrow gap. As far as the potential flow model is concerned, it works well in capturing the resonant frequency, but significantly over-predicts the resonant wave height, mainly due to the ignorance of fluid viscosity and energy dissipation.



(a)  $D=25.2$  cm and  $B_g=5$  cm



(b)  $D=15.3$  cm with  $B_g=7$  cm

Fig. 3 Comparison of non-dimensional wave height with respect to incident wave number at different draft and gap width

Fluid resonance in two narrow gaps between three

identical fixed boxes is also considered in this study. The fixed boxes are defined as Body A, Body B and Body C, respectively, as shown in Fig. 4. The dimensions of water depth  $h=50$  cm, draft  $D=25.2$  cm, breadth of the boxes  $B=50$  cm are set the same as those used the previous cases of twin bodies with single narrow gap. The gap between Body A and Body B is referred to as Gap 1 and that between Body B and Body C is defined as Gap 2. The widths of the two gaps are the same with  $B_g=5$  cm, resulting in  $B_g/B=10\%$ . By using a uniform incident wave height  $H_0=2.4$  cm with  $kh$  varying from 0.79 to 2.92, a total of 59 viscous numerical results are obtained and compared with the experimental data of Iwata et al. (2007) and the boundary element solutions based on potential flow theory. The results are shown in Fig. 5.

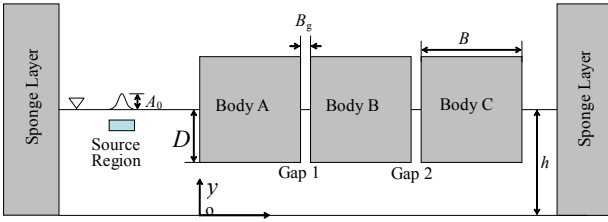


Fig. 4 Sketch definition of three boxes with double narrow gaps

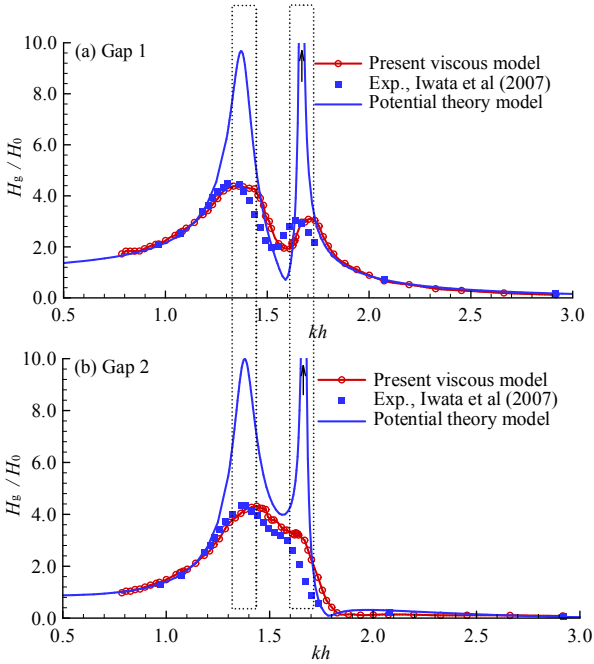


Fig. 5 Comparison of the variations of average wave height with incident wave frequency in Gap 1 and Gap 2

It can be seen from Fig. 5 (a) that the variation of  $H_g/H_0$  with  $kh$  in Gap 1 from viscous flow model agrees well with the experiment data in general but with a small phase lag. The numerical results show that the variation of wave height in Gap 1 has two peak values. This suggests resonance in Gap 1 could take place at two distinct frequencies in contrast to the case of twin bodies with a single narrow gap, where only one resonant frequency was identified. The double-peak variation of  $H_g/H_0$  with  $kh$  is also observed in Gap 2, as shown in Fig. 5 (b), but the second resonant response is not as significant as that in Gap 1. In general, two different resonant frequency bands can be identified for the

present assembly of three bodies with double narrow gaps. The first one is  $1.31 < kh < 1.45$  and the second is  $1.61 < kh < 1.73$ . The resonant bands are indicated approximately by the dashed rectangular in Fig. 5. The existence of two resonant frequency bands is mainly attributed to the presence of two narrow gaps or the intrusion of the third box. From Fig. 5 (a) and (b), one can observe the obvious discrepancy between the results of potential flow model and physical model tests in the band covering the resonant frequencies, although the potential flow model results agree well with the experimental data in the regions far from the resonant frequencies. At the lowest resonant frequency, the potential flow model predicts  $H_g/H_0 \approx 10$ , which is more than two times of the predicted value using the viscous flow model and the measured value. At the highest resonant frequency,  $H_g/H_0 > 30$  is predicted by the potential flow model, which is about 7.5 times of the measured value. It is believed that the over-prediction of  $H_g/H_0$  in the narrow gaps by the potential flow model is due to the ignorance of fluid viscosity, which plays a substantial role in damping the amplitudes of water level oscillations when the fluid resonance takes place. The comparisons demonstrated here suggest that the viscous effects need to be considered in order to obtain satisfactory predictions of water level oscillations in the narrow gaps.

The variations of non-dimensional amplitudes of horizontal forces (normalized by  $\rho gh A_0$  and denoted by  $A_{fx}$ ) with respect to the incident wave frequencies  $kh$  are examined in Fig. 6. A double-peak variation of horizontal forces on Body A and Body C is observed. The force peaks happen around the two fluid resonant frequency bands as illustrated in Fig. 5. However, the variation of  $A_{fx}$  with  $kh$  on Body B has only one peak, which was found to be close to the highest resonant frequency band. Fig. 6 also shows some clues that the horizontal forces on the boxes may correlate closely to the fluid resonance in the narrow gaps. In order to explore the inherent mechanism behind the fluid forces, the water level difference between the opposite sides of the floating structures was investigated. The time-dependent free surface elevation difference is represented by its averaging amplitude,  $A_{ed}$ , normalized by the incident wave height  $H_0$ , as shown in Fig. 6. Note that, the  $A_{ed}$  and  $A_{fx}$  are evaluated in the same time interval for comparison purposes. Fig. 6 (a), (b) and (c) demonstrate the variation of  $A_{ed}$  follows a similar trend to that of  $A_{fx}$  and their peak values appear at the same frequencies. Considering that the horizontal forces are mainly composed of two components, one is resulted from the water level difference between the opposite sides of a body, represented by  $F_d$  herein, and the other is attributed to the fluid/structure interactions, referred to as  $F_i$ . Therefore, it is not surprising to observe the similar variations of  $A_{ed}$  and  $A_{fx}$ . Based on this, one can deduce that the variation of  $F_i$  with  $kh$  may be in a similar manner as that of  $A_{ed}$  or  $A_{fx}$ . In other words, the role of  $F_i$  may compensate the discrepancies between  $A_{fx}$  and  $A_{ed}$ . This speculation is indeed confirmed from Fig. 6, where the large differences between  $A_{fx}$  and  $A_{ed}$  always appear in the resonant regions. Under these situations, the bodies are subjected to the strongest fluid and structure

interactions. That means the contribution of  $F_i$  plays a very important role during the fluid resonance in narrow gaps, while it has rather limited influence on the total horizontal forces as  $kh$  is far from the resonant frequencies. This is demonstrated clearly in this figure. Bearing the above analysis in mind and comparing Fig 6 (a) with Fig 6 (b) and (c), it can be seen that  $F_i$  on Body A is much more significant than that on Body B and Body C since the difference between  $A_{ed}$  and  $A_{fx}$  are more obvious, especially in the high frequency region with short waves. This is in good agreement with the actual physics since Body A is directly exposed to the incident waves, whereas Body B and C are well sheltered by the upstream Body A. Moreover, for short waves, these non-linear interactions are much stronger due to their limited transmitting property. As a result, the strong wave/structure interactions are observed for Body A even outside the resonant bands.

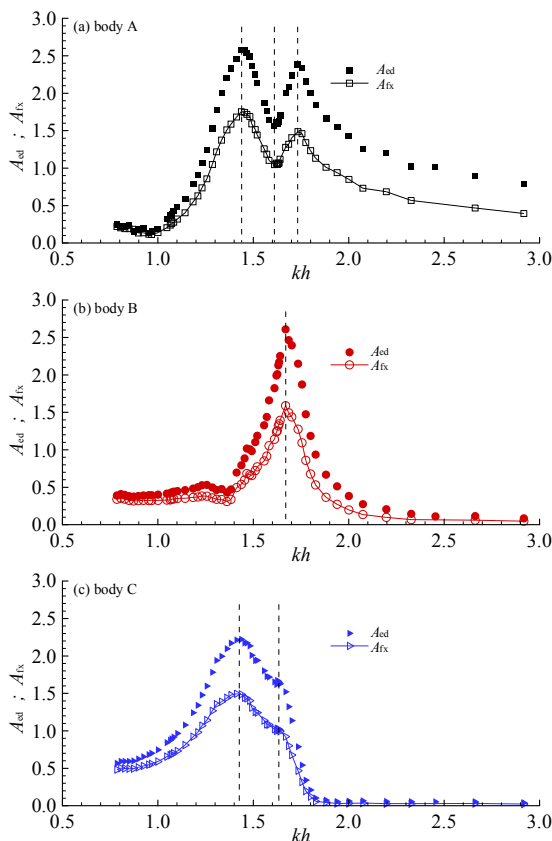


**Fig. 6** Variations of the non-dimensional average amplitudes of water level difference ( $A_{ed}$ ) and the non-dimensional average amplitudes of horizontal forces ( $A_{fx}$ ) with  $kh$

## Conclusion

Numerical simulations of fluid resonance in narrow gaps under water waves are conducted based on both viscous fluid model and potential flow model. The comparisons between numerical results and experimental data confirmed that the potential flow model over-predicts the resonant wave height in narrow gaps, but works equally well as the viscous fluid model in the regions far from the resonant frequencies. Both of the potential and viscous flow models are able to predict resonance frequencies. The mechanisms that are responsible for the predicted horizontal wave forces on

structures were investigated employing the viscous numerical wave flume.

## Reference

- Chen XB. 2005. Hydrodynamic analysis for offshore LNG terminals. The second international workshop on applied offshore hydrodynamics. Rio de Janeiro, Brazil.
- Iwata H, Saitoh T and Miao GP. 2007. Fluid resonance in narrow gaps of very large floating structure composed of rectangular modules. Proceedings of the Fourth International Conference on Asian and Pacific Coasts, Nanjing, China, 2007, 815-826.
- Li BN, Cheng L, Deeks AJ, Teng B. 2005. A modified scaled boundary finite element method for problems with parallel side-faces. Part II. Application and evaluation. Applied Ocean Research, 27: 224-234.
- Lu L, Cheng L, Teng B and Li YC. 2008. Numerical simulation of hydrodynamic resonance in a narrow gap between twin bodies subject to water waves. Proceedings of the Eighteenth International Offshore and Polar Engineering Conference, Vancouver, BC, Canada, July 6-11, 2008, 1: 114-119.
- Lu L, Cheng L, Teng B and Zhao M. 2009. Numerical investigation of fluid resonance in two narrow gaps of three identical rectangular structures. Applied Ocean Research, Accepted and available online.
- Miao GP, Saitoh T, Ishida H. 2001. Water wave interaction of twin large scale caissons with a small gap between. Coastal Engineering Journal, 43(1): 39-58.
- Pauw WH, Huijsmans R and Voogt A. 2007. Advances in the hydrodynamics of side-by-side moored vessels. Proceedings of the 26<sup>th</sup> conference on offshore mechanical and arctic engineering, June 10-15, San Diego, USA.
- Saitoh T, Miao GP and Ishida H. 2006. Theoretical analysis on appearance condition of fluid resonance in a narrow gap between two modules of very large floating structure. Proceedings of the Third Asia-Pacific Workshop on Marine Hydrodynamics, Shanghai, China, 2006, 170-175.
- Sun L, Taylor PH and Eatock Taylor R. 2008. First and second order wave effects in narrow gaps between moored vessels. Proceedings of Marine Operations Specialty Symposium (MOSS), 2008, Singapore.
- Zhu HR, Zhu RC, Miao GP. 2008. A time domain investigation on the hydrodynamic resonance phenomena of 3-D multiple floating structures. Journal of Hydrodynamics, 20(5):611-616.

## Acknowledgment

The first author gratefully acknowledges the financial supports from the Natural Science Foundation of China with Grant No. 50909016, 50921001 and 10802014. Part of the present work was conducted while the first author was visiting The University of Western Australia with the support of ARC Discovery Project Program (Grant No. DP0557060).